International Journal of Pharmaceutics: X 9 (2025) 100326

Contents lists available at ScienceDirect

International Journal of Pharmaceutics: X

journal homepage: www.sciencedirect.com/journal/international-journal-of-pharmaceutics-x

RGD peptide-functionalized micelles loaded with crocetin ameliorate doxorubicin-induced cardiotoxicity

Ting Wang [a,1], Zhimin Li [b,1], Jiawei Lei [a,1], Yuchen Zhang [a], Yingpeng Tong [a], Xingang Guan [a,*], Shuangshuang Wang [a,c,*]

[a] Department of Cardiology, The First People's Hospital of Wenling (Taizhou University Affiliated Wenling Hospital), School of Medicine, Taizhou University, Taizhou 317500, PR China
[b] College of Medical Technology, Beihua University, Jilin 132013, PR China
[c] Key Laboratory of Precision Medicine for Atherosclerotic Diseases of Zhejiang Province, Affiliated First Hospital of Ningbo University, Ningbo 315010, China

ARTICLE INFO

Keywords:
Crocetin
Drug delivery
RGD peptide
Antioxidant effect
Cardiotoxicity

ABSTRACT

Doxorubicin (Dox)-induced cardiotoxicity presents a significant challenge to fully harnessing its chemotherapeutic potential. Crocetin (Cro), a dicarboxylic acid found in the crocus flower and gardenia fruit, has shown remarkable antioxidant and anti-inflammatory activities. However, its poor aqueous solubility and limited cellular uptake severely constrain its further application in treating diseases. In this study, we developed Arg-Gly-Asp (RGD) peptide-decorated nanomicelles delivering Cro to alleviate Dox-induced cardiac injury. The RGD@M (Cro) nanomicelles exhibited excellent aqueous solubility and a drug-loading efficiency of 93.3 %. RGD-decorated micelles could enhance the cellular uptake of Cro in cardiomyocytes and inhibit approximately 60 % of HL-1 cell apoptosis through efficient reactive oxygen species (ROS) scavenging. In a cardiomyopathy mouse model, RGD@M(Cro) substantially reduced cardiac damage and improved cardiac indicators. This study highlights the great potential of RGD-decorated micelles in treating cardiac injury and other diseases.

1. Introduction

Doxorubicin (Dox), a well-known anthracycline, has been widely used as a chemotherapeutic drug due to its excellent cytotoxicity against cancer cells (Kciuk et al., 2023; van der Zanden et al., 2021). Despite its potent tumor-killing effect, Dox treatment always brings severe cardiotoxicity, such as diastolic dysfunction and heart failure, which greatly limits its further application in cancer therapy (Rawat et al., 2021; Wu et al., 2016). Oxidative stress, free radical generation, and cell apoptosis represent the main causes of cardiotoxicity (Robert Li et al., 2024; Sheibani et al., 2022). Alleviating Dox-induced cardiotoxicity remains a critical challenge to fully harnessing the therapeutic potential of Dox in clinical applications (Singh et al., 2023; Zhang et al., 2012; Zhao et al., 2023).

Recently, many natural products have been reported to alleviate cardiotoxicity with different mechanisms (Szponar et al., 2024; Yarmohammadi et al., 2021). Crocetin (Cro), a 20-carbon dicarboxylic acid found in the crocus flower and gardenia fruit, has demonstrated remarkable antioxidant, anti-inflammatory, and anticancer activities (Boozari and Hosseinzadeh, 2022; Guo et al., 2022). Cro can ameliorate cardiotoxicity by inhibiting reactive oxygen species (ROS) production and oxidative stress in cardiomyocytes (Bastani et al., 2022; Hashemi and Hosseinzadeh, 2019). Furthermore, by suppressing the expression of pro-inflammatory factors (such as TNF-α and IL-6) and apoptosis-related genes (including Bcl-2, Bax, and caspase-3), crocetin effectively protects cardiomyocytes from damage (You-Ling et al., 2023; Zhang et al., 2022). Therefore, the ameliorated cardiomyocyte damages of Cro make it a promising candidate for improving the cardiotoxicity induced by Dox or other drugs (Ahmed et al., 2020; Cerdá-Bernad et al., 2022; Dong et al., 2020). Hence, Cro has been widely used to treat inflammatory diseases, neurological disorders and other diseases (Dong et al., 2020; Mehrabani et al., 2020; Zhang et al., 2022). However, the poor aqueous solubility and low internalization greatly limits its further clinical application. Developing novel Cro formulations with good bioavailability holds great promise to improve their therapeutic efficacy (Liu et al., 2023).

Drug delivery systems can improve the delivery efficiency and

* Corresponding authors at: Department of Cardiology, The First People's Hospital of Wenling (Taizhou University Affiliated Wenling Hospital), School of Medicine, Taizhou University, Taizhou 317500, PR China.
E-mail addresses: guanxg@ciac.ac.cn (X. Guan), wangss1023@126.com (S. Wang).
[1] These authors contribute to this work equally.

https://doi.org/10.1016/j.ijpx.2025.100326
Received 6 December 2024; Received in revised form 24 February 2025; Accepted 25 February 2025
Available online 26 February 2025

bioavailability of drugs (Hu et al., 2024; Wang et al., 2022; Wang et al., 2023). Wong K et al. prepared a Cro-γ-cyclodextrin complex and intravenously injected it into mice models to treat Alzheimer's Disease. The complex significantly prevented neuroblastoma cell death from H_2O_2-induced toxicity and promoted Cro crossing the blood-brain barrier to enter the brain (Wong et al., 2020). Nanotechnology opens a new avenue to address the limitations of Cro for improving bioavailability (Mohammadi et al., 2022; Tavasoli et al., 2023). Liu C and his colleagues developed a chitosan nanoparticle delivery system to prevent radio damage. The Cro-crosslinked nanoparticles with good loading efficiency and biocompatibility could extend the blood half-life of Cro in vivo from 10 min to 5 h and significantly alleviate the radiation damage in major organs (Liu et al., 2024). Li H designed a cyclodextrin-based nanosponge to improve the bioavailability of Cro. The Cro-loaded nanosponge showed increased aqueous solubility and enhanced cytotoxicity against tumor cells (Lin et al., 2021). Magnetic nanoparticles delivering Cro demonstrated good release kinetics and enhanced cytotoxicity toward cancer cells compared with free drugs (Ibrahim et al., 2023; Saravani et al., 2020).

Despite the reported advancements in delivery systems, most studies on Cro delivery have primarily focused on improving drug-loading efficiency and validating functions in vitro (Soltani et al., 2024; Taghizadeh et al., 2023). There are limited reports on enhancing the cellular uptake of Cro in cardiomyocytes and demonstrating the protective effects in vivo. Given the increased cellular uptake by integrin stimulation in cardiomyocytes (Schussler et al., 2022), in this study, we fabricated Cro-loaded micelles decorated with Arg-Gly-Asp (RGD) peptide to alleviate Dox-induced cardiotoxicity in heart failure (Scheme 1). The cellular uptake of Cro-loaded micelles as well as their protective effect, reactive oxygen species (ROS) scavenging ability, and cardiomyocyte apoptosis-inhibiting effect were investigated in detail.

2. Materials and methods

2.1. Materials

Cro was obtained from MCE (Shanghai, China). The 4′,6-diamidino-2-phenylindole (DAPI), TUNEL apoptosis assay kit, and reactive oxygen species (ROS) assay kit with CM-H2DCFDA were obtained from Beyotime. Distearoylphosphatidylethanolamine-Poly(ethylene glycol) (DSPE-PEG2000, molecular weight: 2800), DSPE-PEG2000-RGD (molecular weight: 3250), and DSPE-PEG2000-Cy3 (molecular weight: 3383) were purchased from Xian Qiyue. Brain natriuretic peptide (BNP) assay kit was bought from Nanjing Jiancheng Bioengineering Institute (Nanjing, China), and creatine kinase (CK), lactate dehydrogenase (LDH) Zhejiang Century Kangda Medical Technology Co., Ltd. (Hangzhou, China). HL-1 Cardiac Muscle Cell Line was obtained from Haixing Biosciences (Suzhou, China).

2.2. Preparation of Cro-loaded micelles

Cro-loaded micelles M(Cro) were prepared using DSPE-PEG. 5 mg of Cro and 50 mg of DSPE-PEG were dissolved in a 5 mL DMSO. The solution was added dropwise to 10 mL of deionized water. The solution was stirred using a magnetic stirrer at a speed of 200 rpm (rpm). After stirring for 12 h, the solution containing M(Cro) was dialyzed against deionized water to remove DMSO. The dialysis process was carried out for 48 h at room temperature, with the external solution replaced with fresh deionized water every 6 h.The drug loading of Cro in micelles was analyzed by a high-performance liquid chromatography (HPLC) system (Waters e2695) and a Phenomenex Gemini C18 column. The mobile phase consists of methanol-water-glacial acetic acid (75:24.5:0.5, *v/v/v*), with a flow rate of 1.0 mL/min. The column temperature was maintained at 30 °C, and the detection wavelength was set at 423 nm. The injection volume was 20 μL. RGD@M(Cro) micelles were prepared using DSPE-PEG and DSPE-PEG-RGD polymers (molar ratio = 9:1). Cy3-

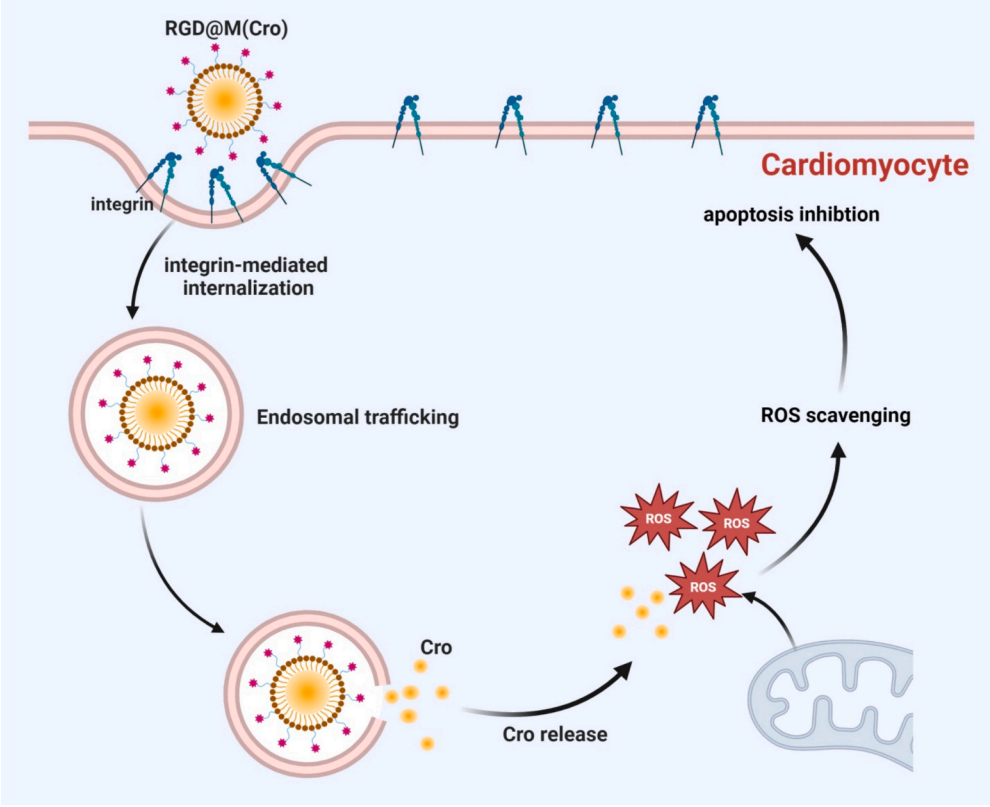

Scheme 1. Schematic illustration of RGD@M(Cro) nanoparticles to alleviate Dox-induced cardiotoxicity.

labeled micelles were acquired using the above protocols.

2.3. Characterization of Cro-loaded micelles

The size analysis of M(Cro) and RGD@M(Cro) were analyzed by dynamic light scattering (DLS). The surface charge of Cro-loaded micelles was determined using a size and zeta potential meter (Microtrac, Nanotrac Wave II). For morphology analysis, nanoparticles were dropped on glow-discharged carbon-coated copper grids and then negatively stained with 2 % uranyl acetate. The morphology of Cro-loaded micelles was analyzed with a JEM 1011 microscope (JEOL, Japan).

2.4. Cultivation of HL-1 Cells

The HL-1 cell line, derived from mouse cardiomyocytes, was acquired from Haixing Biosciences located in Suzhou, China. These cells were maintained in a growth-promoting environment consisting of Dulbecco's Modified Eagle Medium (DMEM) supplemented with 10 % fetal bovine serum (FBS) at a temperature of 37 °C and under a 5 % carbon dioxide (CO_2) atmosphere. To ensure optimal growth conditions, the cells were passaged when they reached 70 to 80 % confluence. The HL-1 cells underwent a pretreatment regimen involving exposure to 5 μM of Dox and different Cro formulations (Cro, M(Cro), or RGD@M (Cro)) for 24 h.

2.5. In vitro studies

2.5.1. Cellular uptake

The cellular uptake of Cro-loaded micelles was analyzed using confocal laser scanning microscopy (CLSM) imaging and flow cytometry analysis. Cy3-labeled M(Cro) and RGD@M(Cro) micelles, incorporating 20 μM Cro, were prepared and added to the HL-1 cells for 2 h at 37 °C. After washing with PBS, HL-1 cells were stained with DAPI for 15 min. The uptaken micelles by HL-1 cells were analyzed by CLSM (Zeiss, LSM710). As for the flow cytometry assay, HL-1 cells treated with Cro micelles were digested with trypsin and washed with PBS. The suspension was subjected to flow cytometry analysis (gated at the PI channel).

2.5.2. CCK8 assay

The protective effect of Cro-loaded micelles was examined in HL-1 cells by CCK8 assay. HL-1 cells were seeded into 96-well plates at a density of 5×10^3 per well and cultured at 37 °C for 24 h. On the second day, the medium was replaced with fresh medium containing Dox + Cro, Dox + M(Cro), or Dox + RGD@M(Cro) with different Cro concentrations (0, 2.5, 5, 10, 20, 40 μM). After two days of incubation, CCK-8 solution was added and incubated for 2 h. The solution absorbance was measured on a microplate reader (TECAN, M200) at 450 nm. Experiments were repeated three times.

2.5.3. Reactive oxygen species (ROS) analysis

The generation of intracellular ROS was quantitatively determined using the fluorescent probe 2′,7′-dichlorofluorescein diacetate (DCFH-DA) kits (Beyotime, China). Cells were seeded in 12-well plates and subsequently incubated with DCFH-DA for 30 min to allow for its permeation and conversion into the fluorescent product by ROS within the cells. Following incubation, the cells were thoroughly rinsed to remove any excess probe and then examined under a confocal microscope (Olympus BX53) to capture fluorescent images. The level of apoptosis, indirectly indicated by the intensity of green fluorescence (representing ROS levels), was quantitatively evaluated as the ratio of green fluorescent areas to the total number of nuclei stained with DAPI, providing a direct visualization and quantification of ROS-mediated cellular stress.

2.5.4. TUNEL analysis

HL-1 Cells were seeded in 12-well plates and treated with PBS, Dox, Dox + Cro, Dox + M(Cro), or Dox + RGD@M(Cro) containing equal Cro (40 μM). After 24 h of incubation, the cells were washed with PBS and treated with Terminal deoxynucleotidyl transferase-mediated dUTP Nick-End Labeling (TUNEL) (Beyotime, China). After washing, the stained cells were imaged using fluorescent microscopy. As for the tissue staining of TUNEL, the heart tissues of mice were excised and preserved in 10 % phosphate-buffered formalin solution for a duration of 24 h to ensure proper fixation. Following this, the samples were embedded in paraffin wax and sectioned into thin slices of approximately 4 to 5 μm in thickness. The slices were then subjected to the TUNEL staining procedure, utilizing the TUNEL BrightGreen Apoptosis Detection Kit in strict adherence to the manufacturer's guidelines. During this process, apoptotic nuclei were fluorescently labeled with a bright green stain, while all cardiomyocyte nuclei were counterstained with DAPI for visualization. The prepared heart tissue sections were subsequently examined under a confocal microscope (Olympus, BX53) to capture images. The extent of apoptosis was quantitatively assessed as the proportion of TUNEL-positive nuclei relative to the total number of DAPI-stained nuclei.

2.6. In vivo studies

All the mice were acclimatized to the environment for a week before the commencement of the experiment. The study was conducted in full compliance with ethical standards for research animals and was approved by the Animal Ethics Committee at the Experimental Animal Institute of Taizhou University (TZXY-2023-20231053).

2.6.1. Echocardiography analysis in vivo

18–20 g male C57BL/6 mice were bought from Zhejiang Vital River Company in Hangzhou, China. They were housed under 12-h light/dark cycles and provided with unlimited access to food and water. Group 1 (Normal Group): Received saline treatment. Group 2 (Model Group): Administered Dox (15 mg/kg, ip) on the seventh day. Group 3 (Dox + Cro Group): Treated with Dox (15 mg/kg) and Cro (20 mg/kg, ip) daily for one week. Group 4 (Dox + M(Cro) Group): Administered Dox (15 mg/kg) and M(Cro) (20 mg/kg, ip) daily for one week. Group 5 (Dox + RGD@M(Cro) Group): Treated with Dox (15 mg/kg) and RGD@M(Cro) (20 mg/kg, ip) daily for one week. In the Cardiovascular Assessment Facility, transthoracic echocardiography was conducted on six mice from each group using the advanced Mylab SigmaVet ultrasound system equipped with the SL3116 probe manufactured by Esaote in Genoa, Italy. This non-invasive procedure allowed for the acquisition of standard views to precisely measure the left ventricular (LV) end-diastolic diameter (LVEDD) and end-systolic diameter (LVESD). These measurements served as the basis for deriving key cardiac functional parameters, including LV stroke volume, ejection fraction, and cardiac output, which were calculated from the end-diastolic and end-systolic LV volumes.

Furthermore, Doppler echocardiography was employed to record the mitral valve's *E*-wave and A-wave from an apical four-chamber view of the LV. This analysis provided insights into mitral valve function. Additionally, tissue Doppler imaging was utilized to measure the lateral annulus velocity of the mitral valve (lateral E0), offering a detailed assessment of myocardial tissue dynamics. Throughout the echocardiographic procedure, the mice were maintained under mild anesthesia, achieved through the administration of 1–1.5 % Isoflurane, ensuring their comfort and minimizing any potential stress on the cardiovascular system during the examination.

2.6.2. H&E and Masson staining

Subsequently, mouse serum and heart were collected after the mice were anesthetized. The hearts were taken out and were fixed in 4 % tissue cell fixative (4 % paraformaldehyde) for 24 h, dehydrated by an automatic dehydrator for 16 h, and then routinely embedded in a paraffin embedding machine for preparation of heart tissue sections. H&E and Masson staining were performed according to the reported

methods.

2.6.3. Detection of BNP, CK, and LDH

Serum brain natriuretic peptide (BNP) was detected by Assay Kits according to the standard procedure of Assay Kit (Nanjing Jiancheng Bioengineering Institute), Serum creatine kinase (CK) and lactate dehydrogenase (LDH) were detected by a fully automated biochemical analyzer Toshiba FR40 according to the procedure, and quality control was performed on the biochemical analyzer before use.

2.7. Statistical analysis

All the reported data are shown as the mean ± standard deviation. Statistical analysis was performed using SPSS software. One-way or two-way analysis of variance (ANOVA) and Tukey post hoc tests were used to calculate the statistical significance. The log-rank test was used to determine the survival of mice. Statistical significance is indicated as follows: $^{*}P < 0.05$, $^{**}P < 0.01$.

3. Results and discussions

3.1. Preparation of Cro-loaded micelles

To address the issue of poor aqueous solubility of Cro, we selected FDA-approved PEG-DSPE material to prepare micelles as the nanocarrier. It has been reported that integrin stimulation can enhance the cellular uptake of macromolecules by cardiomyocytes (Kumar et al., 2023; Swildens et al., 2011). It is reported that RGD peptides could selectively bind with integrin to enhance the internalization of macromolecules and nanoparticles (Alipour et al., 2020; Swildens et al., 2011). Therefore, in this study, we decorated the Cro micelles with RGD peptides to promote cellular uptake (Fig. 1A). TEM results indicated that RGD@M(Cro) had a solid spherical nanostructure (Fig. 1B). RGD-functioned micelles (RGD@M(Cro)) have a mean diameter of 203.9 nm, a little bigger than that of Cro micelles without RGD (179.9 nm) (Fig. 1C). The surface charge of RGD@M(Cro) and M(Cro) was determined to be −18.7 and − 12.2 mV, respectively (Fig. 1D). M(Cro) and RGD@M(Cro) nanomicelles exhibit drug loading efficiencies of 94.7 % and 93.3 %, respectively.

3.2. RGD decoration enhanced cellular uptake of Cro-loaded micelles

To enhance the cellular uptake of Cro micelles, we decorated the Cro nanoparticles with RGD peptides on their surface. The uptake of Cro micelles in HL-1 cardiomyocytes was analyzed using confocal laser scanning microscopy (CLSM). The micelles were labeled with a Cy3 fluorescent dye to track their internalization. As shown in Fig. 2A, M (Cro) nanoparticles were successfully taken up by cardiomyocytes, displaying cytoplasmic fluorescent spots. In contrast to the slight fluorescence observed in the M(Cro) group, the increased fluorescence was observed in HL-1 cells treated with the RGD@M(Cro) group. Enhanced cellular uptake of RGD-decorated micelles can be attributed to the specific binding of the RGD peptide to integrin receptors that are expressed on the surface of cardiomyocytes. This receptor-mediated endocytosis facilitates a more efficient internalization of RGD-decorated nanomicelles compared to non-targeted micelles (Swildens et al., 2011). Additionally, we performed flow cytometry analysis to further assess micelle internalization (Fig. 2B). RGD@M(Cro) demonstrated superior internalization in HL-1 cells compared to M(Cro)-treated cells, suggesting enhanced uptake of RGD-decorated micelles by cardiomyocytes.

3.3. RGD@M(Cro) nanoparticles significantly alleviated Dox-induced cardiotoxicity

In light of the antioxidant activity of Cro, we investigated whether Cro micelles have a protective effect in alleviating Dox-induced cytotoxicity. HL-1 cells were treated with Dox to simulate in vitro cardiotoxicity. Dox at a concentration of 5 μM can kill half of the cells, so it was selected for subsequent time-course experiments. The

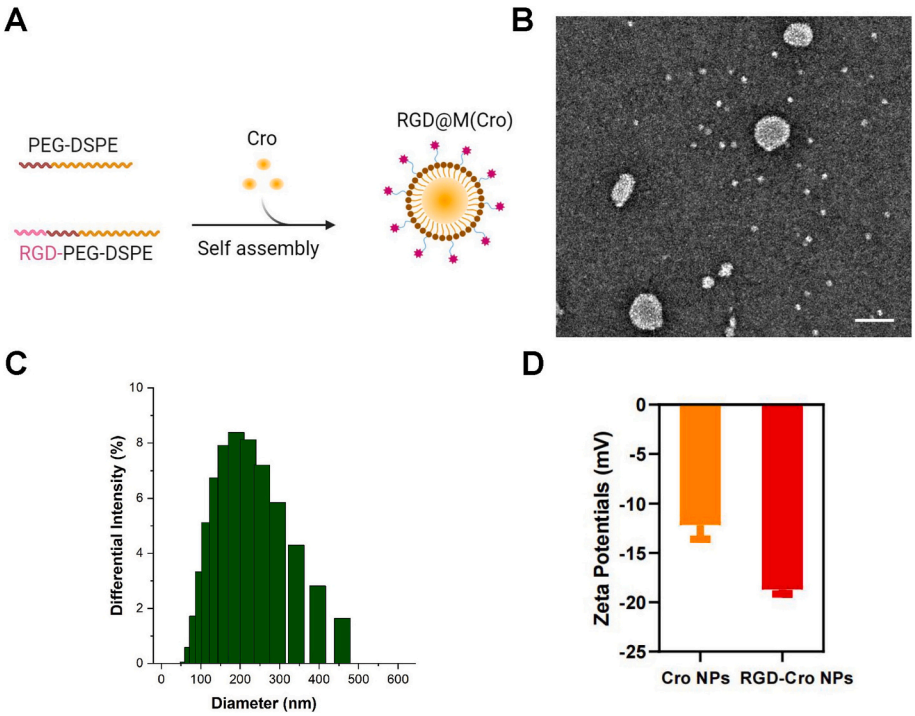

Fig. 1. Preparation and characterization of RGD@M(Cro). A: Schematic illustration of RGD@M(Cro) preparation. B: Morphology analysis of RGD@M(Cro) nanomicelles detected by TEM. Scale bar: 100 nm. C: Size distribution of RGD@M(Cro) determined by dynamic light scattering (DLS). D: Zeta potential analysis of RGD@M(Cro) micelles.

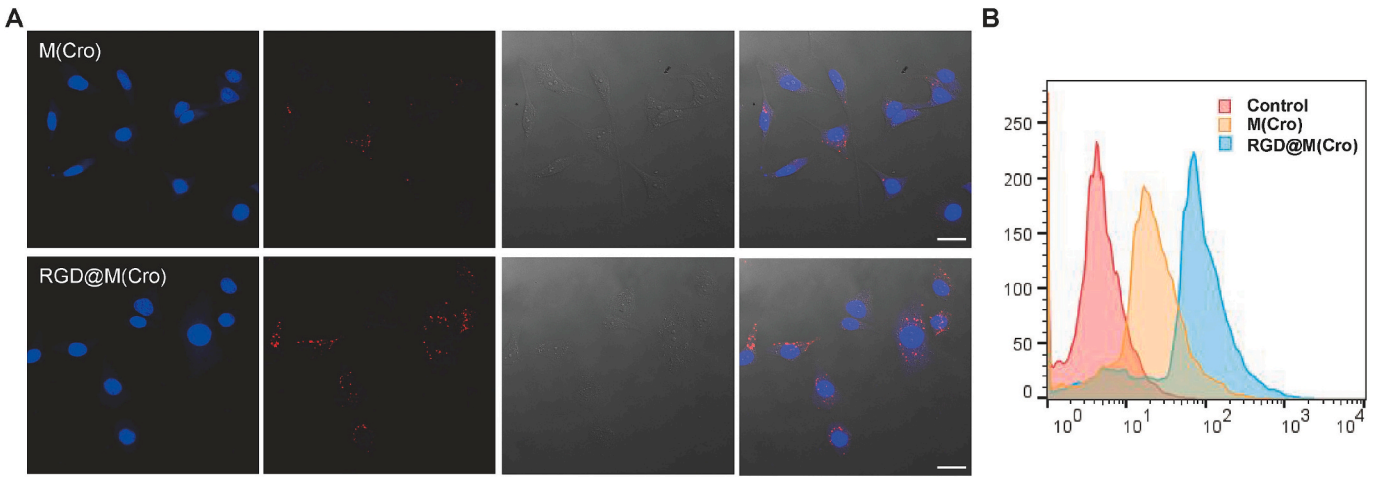

Fig. 2. Cellular uptake of RGD@M(Cro) nanoparticles in HL-1 cells. A: The internalization of RGD@M(Cro) nanoparticles in HL-1 cells by CLSM imaging. Cy3-labeled M(Cro) or RGD@M(Cro) nanoparticles containing equal Cro (20 μM) were incubated with HL-1 cells for 2 h. Scale bar: 10 μm. B: Flow cytometric analysis of HL-1 cells treated with M(Cro) or RGD@M(Cro) nanomicelles containing 20 μM Cro for 2 h at 37 °C.

cytoprotective effects of Cro micelles were analyzed using the CCK-8 assay. The results indicated that Cro, M(Cro), and RGD@M(Cro) enhanced cell viability at all tested concentrations (Fig. 3A). As a small molecule drug, Cro could penetrate into cardiomyocytes and exert protecting effect in vitro. RGD@M(Cro) micelles treatment protected more HL-1 cells from cytotoxicity compared to the M(Cro) micelle group. Given induced regulated cell death by Dox (Christidi and Brunham, 2021), we further examined whether RGD@M(Cro) micelles alleviated cardiotoxicity by inhibiting cell apoptosis of cardiomyocytes. The TUNEL assay was employed to assess cell apoptosis in cardiomyocytes. CLSM imaging demonstrated that free Cro and Cro micelles inhibited Dox-induced apoptosis with different degrees of protection (Fig. 3B). Compared to the bright fluorescence observed in the Dox and Cro group, significantly reduced green fluorescence was detected in the RGD@M (Cro) micelles group (Fig. 3C). These results demonstrated that RGD@M (Cro) exhibited a more potent apoptosis-inhibiting effect than the M (Cro) group. This superior efficacy of RGD@M(Cro) can be attributed to the enhanced internalization of Cro in cardiomyocytes, facilitated by RGD decoration. The increased uptake of RGD-decorated Cro micelles ultimately contributed to the enhanced apoptosis inhibitory effect. To elucidate the mechanisms underlying the suppression of cell apoptosis, we further evaluated the ROS scavenging ability of RGD@M(Cro) micelles in HL-1 cells. Dox treatment induced significant ROS production in HL-1 cells, while RGD@M(Cro) micelles markedly decreased ROS accumulation in cardiomyocytes, ultimately leading to reduced apoptosis (Fig. 3D).

3.4. RGD@M(Cro) nanoparticles significantly improved heart tissue damages in vivo

To determine whether RGD@M(Cro) plays a similar protective role in reducing cardiotoxicity, we developed a cardiomyopathy mouse model by administering a single 15 mg/kg dose of doxorubicin. Cardiac performance was assessed using echocardiography. The echocardiographic results revealed severe cardiac damage following Dox treatment, whereas Cro, M(Cro), and RGD@M(Cro) significantly mitigated cardiac injuries in the mice (Fig. 4A). Notably, both M(Cro) and RGD@M (Cro) effectively reversed the Dox-mediated reductions in ejection fraction (EF) (Fig. 4B) and fractional shortening (FS) (Fig. 4C), while also improving left ventricular end-diastolic diameter (LVEDd) (Fig. 4D) and left ventricular end-systolic diameter (LVESd) (Fig. 4E). The results of the echocardiography (depicted in Fig. 1) showed that administering Dox caused cardiac dysfunction in mice. Compared with M(Cro) micelles, RGD@M(Cro) led to a notable in their cardiac function. Additionally, the indices (EF%, FS%, LVEDd, and LVESd) in RGD@M (Cro) group demonstrated potent therapeutic efficacy in alleviating heart tissue damages.

We further evaluated the protective effect of RGD@M(Cro) using histological staining. Dox treatment led to significant changes in heart structure, including increased intercellular spaces and the formation of vacuoles (indicated by arrows), indicating induced toxicity (Fig. 5A and B). Notably, treatment with RGD@M(Cro) effectively mitigated these structural alterations in cardiomyocytes (Fig. 5A and B). Additionally, RGD@M(Cro) treatment significantly reduced the occurrence of fibrosis, as demonstrated by Masson's staining analysis (Fig. 5C). Furthermore, the preemptive administration of RGD@M(Cro) markedly decreased both pathological damage and cardiac fibrosis caused by Dox. TUNEL staining results revealed a higher incidence of cardiac cell apoptosis in the Dox group, whereas RGD@M(Cro) substantially attenuated the severity of myocardial cell apoptosis (Fig. 5D). To further assess cardiac injuries, we analyzed some pivotal indicators of cardiac function, including brain natriuretic peptide (BNP), creatine kinase (CK), and lactate dehydrogenase (LDH). BNP is a hormone secreted by the heart that plays a crucial role in fluid balance and blood pressure regulation. Elevated CK levels in the blood can indicate tissue damage, particularly in myocardial infarction. Compared to the increased levels of BNP (Fig. 5E), CK (Fig. 5F), and LDH (Fig. 5G) observed in the Dox group, Cro or Cro-loaded micelles significantly decreased these values, suggesting a clear protective effect against Dox-induced injuries. Specifically, RGD@M(Cro) and M(Cro) demonstrated superior performance compared to the crocetin group. In summary, this compelling evidence collectively indicates that RGD@M(Cro) possesses the capability to mitigate Dox-induced myocardial injury in vivo.

4. Discussions

Crocetin, a natural compound derived from crocin or other plant sources, exhibits a wide range of multifunctional properties, including cardioprotective, neuroprotective, and anticancer effects (Guo et al., 2022). It has been shown to improve outcomes in various cardiovascular diseases, such as hypertension, myocardial ischemia, and atherosclerosis. For example, crocetin reduces oxidative stress induced by reactive oxygen species (ROS), thereby contributing to the management of hypertension (Yoshino et al., 2011). In the context of myocardial ischemia, crocetin has been demonstrated to suppress intracellular ROS production, attenuate cardiomyocyte apoptosis, and lower plasma levels of inflammatory mediators, including tumor necrosis factor (TNF)-α, interleukin (IL)-6, and IL-1β (Liu et al., 2020). Furthermore, crocetin

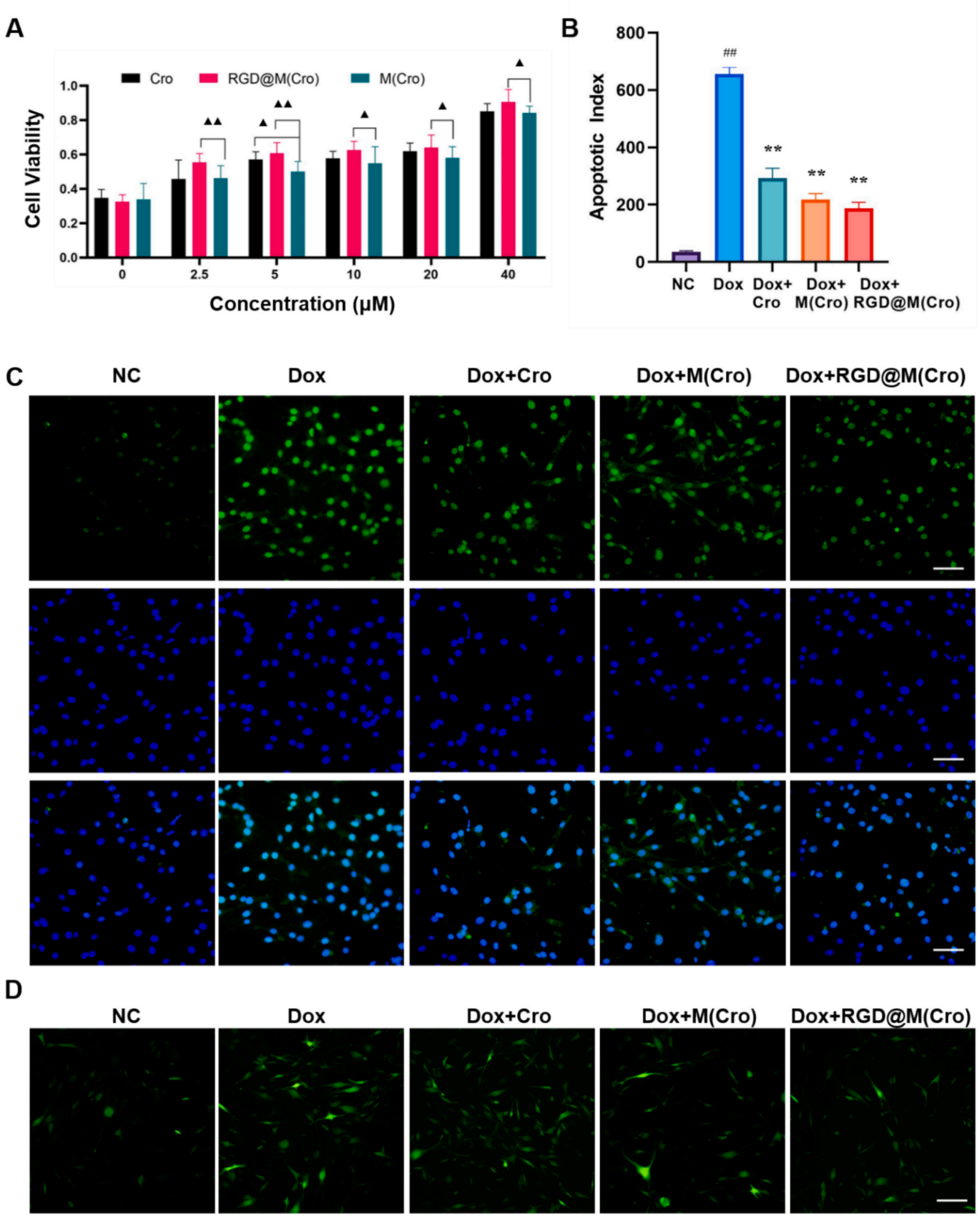

Fig. 3. RGD@M(Cro) nanoparticles alleviated cardiotoxicity in HL-1 cells. A: The protective analysis of RGD@M(Cro) nanoparticles containing different Cro centrations (0, 2.5, 5, 10, 20, 40 μM) in HL-1 cells via CCK8 assay. B: Quantitive analysis of apoptotic cells in TUNEL analysis. C: TUNEL analysis of cell apoptosis treated with Cro, M(Cro), or RGD@ M(Cro) containing 40 μM Cro. Scale bar: 100 μm. D: ROS scavenging analysis of Cro, M(Cro), or RGD@M(Cro) micelles containing 40 μM Cro. Scale bar: 20 μm. Statistical significance is indicated as follows: $^{*}P < 0.05$, $^{**}P < 0.01$ compared to the Dox group; $^{\#\#}P < 0.01$ compared to the Normal Group.$^{\blacktriangle}P < 0.05$, $^{\blacktriangle\blacktriangle}P < 0.01$ compared to the M(cro) group.

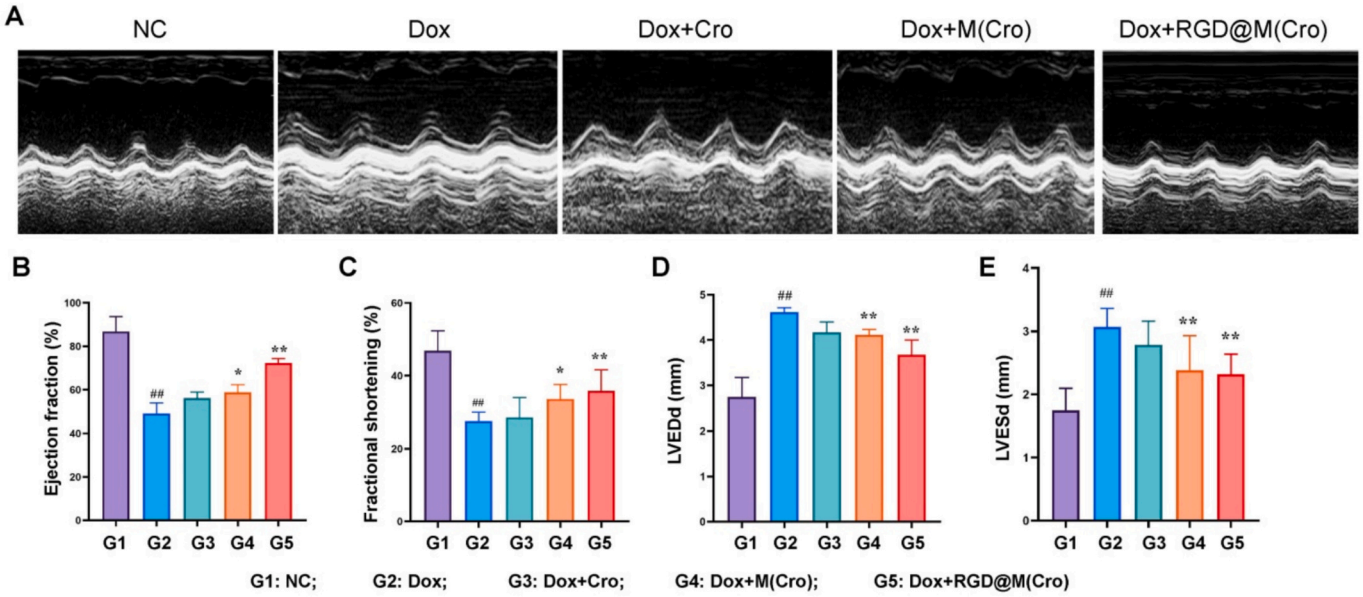

Fig. 4. RGD@M(Cro) nanoparticles alleviated Dox-induced cardiac damage in vivo. The mice were administered Cro, M(Cro), or RGD@M(Cro) (20 mg/kg) for one week, followed by a single intraperitoneal injection of Dox (15 mg/kg) on the seventh day. A: Representative echocardiographic images in mice treated with G1 (Control), G2(Dox), G3(Dox + Cro), G4(Dox + M(Cro)), G5(Dox + RGD@M(Cro)). B: Ejection fraction (EF%) analysis in different groups; C: Fractional shortening (FS %) analysis in different groups; D: Left ventricular end-diastolic diameter (LVEDd) analysis; E: Left ventricular end-systolic diameter (LVESd) analysis. All data are reported as mean ± standard deviation (SD), with $n = 6$ mice per group. Statistical significance is indicated as follows: $^{*}P < 0.05$, $^{**}P < 0.01$ compared to the Dox group; $^{\#\#}P < 0.01$ compared to the Normal Group.

plays a pivotal role in the prevention and treatment of other cardiovascular conditions, such as arrhythmia, myocardial infarction, cardiac insufficiency, myocarditis, and atherosclerosis, through diverse molecular mechanisms (Guo et al., 2022).

Despite its promising cardioprotective properties, the clinical application of crocetin is significantly limited by its poor oral bioavailability and suboptimal pharmacokinetic profile (Liu and Qian, 2002; Xi et al., 2007). To address these challenges, the development of advanced drug delivery systems—such as nanoparticles, liposomes, or prodrug formulations—has emerged as a promising strategy to enhance the therapeutic efficacy of crocetin in treating cardiovascular and other diseases (Huang et al., 2019; Prieložná et al., 2024). In this study, we utilized FDA-approved poly (ethylene glycol)-distearoylphosphatidylethanolamine (PEG-DSPE) block copolymers to design nanomicelles for the safe and effective delivery of crocetin (Cro). Additionally, we functionalized the nanocarrier with the RGD (Arg-Gly-Asp) peptide, which exhibits high affinity for integrin receptors, to facilitate the targeted delivery of crocetin to cardiomyocytes (Schussler et al., 2022). Given the abundant expression of integrin receptors on cardiomyocyte surfaces (Zhang et al., 2024), RGD-decorated nanomicelles are expected to selectively bind to these receptors, enhancing cellular internalization and increasing intracellular crocetin concentrations. Notably, RGD@M(Cro) nanoparticles demonstrated superior anti-apoptotic activity compared to the non-targeted M(Cro) group, ultimately contributing to the mitigation of cardiac damage in vivo. While this study demonstrates the potential of RGD-decorated nanomicelles for the targeted delivery of crocetin to cardiomyocytes, there are several limitations to be addressed. First, although RGD-decoration enhances targeting efficiency through integrin receptor binding, the potential off-target effects of RGD@M(Cro) nanoparticles on other cell types were not investigated in this study. This could impact the specificity and safety profile of the nanocarrier. Second, despite the anti-apoptotic effects of RGD@M(Cro) nanoparticles, the underlying molecular mechanisms were not explored in depth. A more detailed mechanistic investigation would provide deeper insights into the therapeutic potential of this delivery system. Addressing these limitations in future studies will be essential to advance the development of crocetin-based nanomedicines for cardiovascular diseases.

5. Conclusion

In this study, we developed RGD-decorated Cro micelles to alleviate Dox-induced cardiotoxicity. In addition to excellent aqueous solubility and drug-loading efficiency, RGD@M(Cro) nanomicelles demonstrated good cellular uptake and efficiently inhibited cell apoptosis in HL-1 cells through ROS scavenging. In a cardiomyopathy mouse model, RGD@M (Cro) treatment significantly mitigated cardiac damage, demonstrating its promising potential for clinical applications.

Funding

This study was supported by Zhejiang Provincial Natural Science Foundation of China (LY23C100001, LQ22H280014), National Natural Science Foundation of China (81703688), Zhejiang Provincial Medical and Health Program (2023KY411, 2025KY467, 2025KY1880), Science and Technology Program of Taizhou City (21ywb115, 22gya03, 24ywa54), Collaborative Innovation Center of Research and Development on the Whole Industry Chain of Yu-Yao, Henan Province (2024YYXT-KFKT-03).

CRediT authorship contribution statement

Ting Wang: Investigation. **Zhimin Li:** Investigation. **Jiawei Lei:** Investigation. **Yuchen Zhang:** Investigation. **Yingpeng Tong:** Investigation. **Xingang Guan:** Writing – review & editing, Writing – original draft, Project administration. **Shuangshuang Wang:** Writing – review & editing, Funding acquisition.

Declaration of competing interest

The authors declare that they have no known competing financial interests or personal relationships that could have appeared to influence the work reported in this paper.

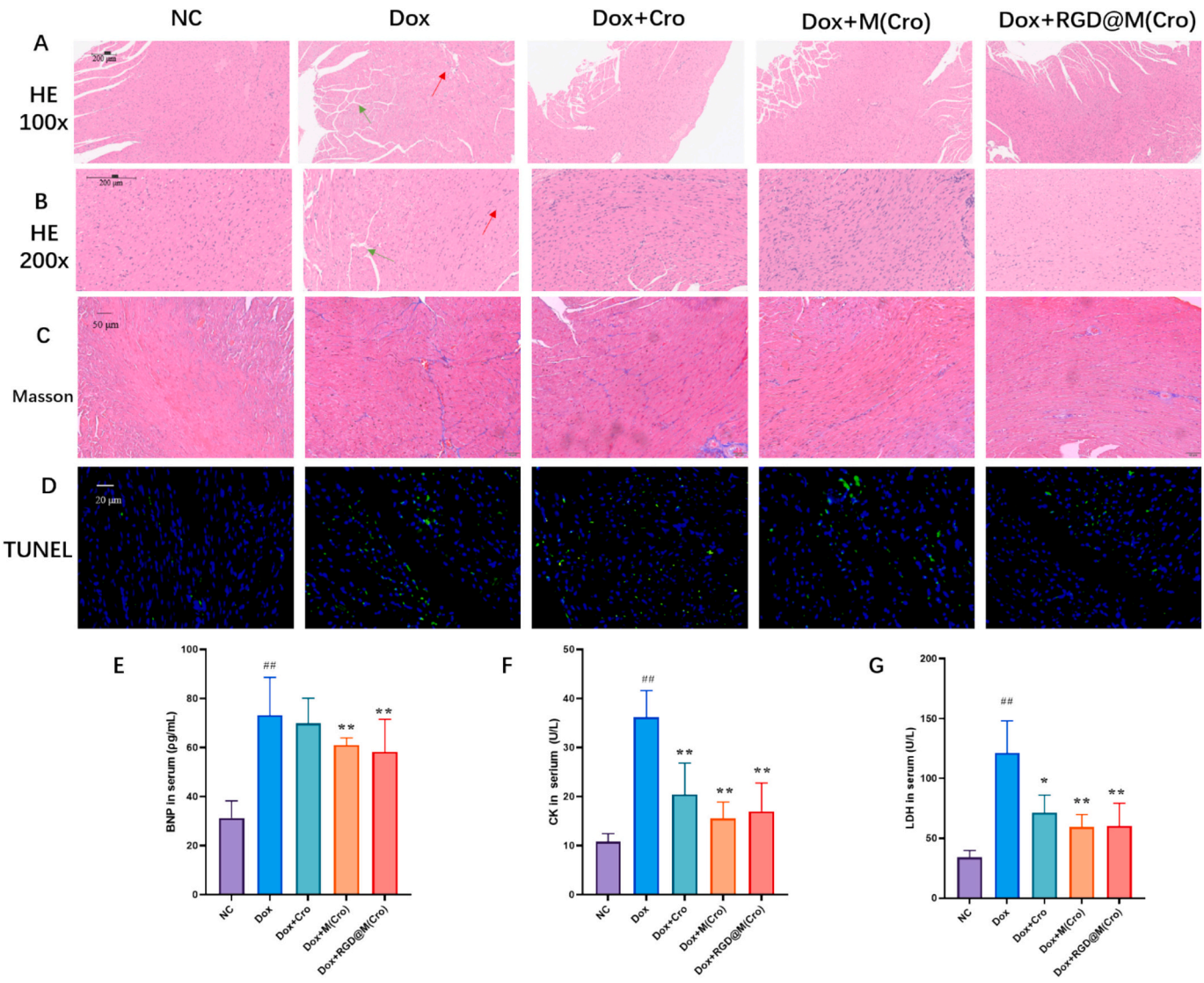

Fig. 5. RGD@M(Cro) nanoparticles on cardiac tissue staining and detection of cardiac injury indicators. The mice were administered Cro, M(Cro), or RGD@M(Cro) (20 mg/kg) for one week, followed by a single intraperitoneal injection of Dox (15 mg/kg) on the seventh day. A&B: H&E staining; C: Masson staining; D: TUNEL staining of cardiac tissue in mice. Serum BNP(E), CK (F), and LDH (G) of Dox-induced cardiotoxicity in mice. Data are presented as mean ± SD; n = 6, $^{*}P < 0.05$, $^{**}P < 0.01$ compared with the Dox group, $^{\#\#}P < 0.01$ compared with Normal Group. The red arrow represents inflammatory cell infiltration, and the green arrow represents myocardial cell arrangement. (For interpretation of the references to colour in this figure legend, the reader is referred to the web version of this article.)

Data availability

Data will be made available on request.

References

Ahmed, S., Hasan, M.M., Heydari, M., Rauf, A., Bawazeer, S., Abu-Izneid, T., Rebezov, M., Shariati, M.A., Daglia, M., Rengasamy, K.R., 2020. Therapeutic potentials of crocin in medication of neurological disorders. Food Chem. Toxicol. 145, 111739. https://doi.org/10.1016/j.fct.2020.111739.

Alipour, M., Baneshi, M., Hosseinkhani, S., Mahmoudi, R., Jabari Arabzadeh, A., Akrami, M., Mehrzad, J., Bardania, H., 2020. Recent progress in biomedical applications of RGD-based ligand: from precise cancer theranostics to biomaterial engineering: a systematic review. J. Biomed. Mater. Res.t A 108, 839–850. https://doi.org/10.1002/jbm.a.36862.

Bastani, S., Vahedian, V., Rashidi, M., Mir, A., Mirzaei, S., Alipourfard, I., Pouremamali, F., Nejabati, H., Maroufi, N.F., Akbarzadeh, M., 2022. An evaluation on potential anti-oxidant and anti-inflammatory effects of crocin. Biomed. Pharmacother. 153, 113297. https://doi.org/10.1016/j.biopha.2022.113297.

Boozari, M., Hosseinzadeh, H., 2022. Crocin molecular signaling pathways at a glance: a comprehensive review. Phytother. Res. 36, 3859–3884. https://doi.org/10.1002/ptr.7583.

Cerdá-Bernad, D., Valero-Cases, E., Pastor, J.-J., Frutos, M.J., 2022. Saffron bioactives crocin, crocetin and safranal: effect on oxidative stress and mechanisms of action. Crit. Rev. Food. Sci. 62, 3232–3249. https://doi.org/10.1080/10408398.2020.1864279.

Christidi, E., Brunham, L.R., 2021. Regulated cell death pathways in doxorubicin-induced cardiotoxicity. Cell Death & Disease 12, 339.

Dong, N., Dong, Z., Chen, Y., Gu, X., 2020. Crocetin alleviates inflammation in MPTP-induced Parkinson's disease models through improving mitochondrial functions. Parkinsons Dis. 2020, 9864370. https://doi.org/10.1155/2020/9864370.

Guo, Z.-L., Li, M.-X., Li, X.-L., Wang, P., Wang, W.-G., Du, W.-Z., Yang, Z.-Q., Chen, S.-F., Wu, D., Tian, X.-Y., 2022. Crocetin: a systematic review. Front. Pharmacol. 12, 745683. https://doi.org/10.3389/fphar.2021.745683.

Hashemi, M., Hosseinzadeh, H., 2019. A comprehensive review on biological activities and toxicology of crocetin. Food Chem. Toxicol. 130, 44–60. https://doi.org/10.1016/j.fct.2019.05.017.

Hu, N., Xue, H., Zhang, T., Fan, Y., Guo, F., Li, Z., Huo, M., Guan, X., Chen, G., 2024. Harnessing PD-1 cell membrane-coated paclitaxel dimer nanoparticles for potentiated chemoimmunotherapy. Biomed. Pharmacother. 174, 116482. https://doi.org/10.1016/j.biopha.2024.116482.

Huang, Z.-G., Lv, F.-M., Wang, J., Cao, S.-J., Liu, Z.-P., Liu, Y., Lu, W.-Y., 2019. RGD-modified PEGylated paclitaxel nanocrystals with enhanced stability and tumor-targeting capability. Int.J Pharm. 556, 217–225. https://doi.org/10.1016/j.ijpharm.2018.12.023.

Ibrahim, S., Baig, B., Hisaindee, S., Darwish, H., Abdel-Ghany, A., El-Maghraby, H., Amin, A., Greish, Y., 2023. Development and evaluation of crocetin-functionalized pegylated magnetite nanoparticles for hepatocellular carcinoma. Molecules 28, 2882. https://doi.org/10.3390/molecules28072882.

Kciuk, M., Gielecińska, A., Mujwar, S., Kołat, D., Kałuzińska-Kołat, Ż., Celik, I., Kontek, R., 2023. Doxorubicin—an agent with multiple mechanisms of anticancer activity. Cells 12, 659. https://doi.org/10.3390/cells12040659.

Kumar, V.B., Tiwari, O.S., Finkelstein-Zuta, G., Rencus-Lazar, S., Gazit, E., 2023. Design of functional RGD peptide-based biomaterials for tissue engineering. Pharmaceutics 15, 345. https://doi.org/10.3390/pharmaceutics15020345.

Lin, S., Li, Q., Jiang, S., Xu, Z., Jiang, Y., Liu, L., Jiang, J., Tong, Y., Wang, P., 2021. Crocetin ameliorates chronic restraint stress-induced depression-like behaviors in mice by regulating MEK/ERK pathways and gut microbiota. J. Ethnopharmacol. 268, 113608. https://doi.org/10.1016/j.jep.2020.113608.

Liu, T., Qian, Z., 2002. Pharmacokinetics of crocetin in rats. Acta Pharm. Sin. 37, 367–369. https://doi.org/10.16438/j.0513-4870.2002.05.012.

Liu, P., Xue, Y., Zheng, B., Liang, Y., Zhang, J., Shi, J., Chu, X., Han, X., Chu, L., 2020. Crocetin attenuates the oxidative stress, inflammation and apoptosis in arsenic trioxide-induced nephrotoxic rats: Implication of PI3K/AKT pathway. Int. Immunopharmacol. 88, 106959. https://doi.org/10.1016/j.intimp.2020.106959.

Liu, N., Xiao, J., Zang, L.-H., Quan, P., Liu, D.-C., 2023. Preparation of trans- crocetin with high solubility, stability, and oral bioavailability by incorporation into three types of cyclodextrins. Pharmaceutics 15, 2790. https://doi.org/10.3390/pharmaceutics15122790.

Liu, C., Wang, L., Zhou, Y., Xia, W., Wang, Z., Kuang, L., Hua, D., 2024. Biogenic crocetin-crosslinked chitosan nanoparticles with high stability and drug loading for efficient radioprotection. Int. J. Biol. Macromol. 265, 130756. https://doi.org/10.1016/j.ijbiomac.2024.130756.

Mehrabani, M., Goudarzi, M., Mehrzadi, S., Siahpoosh, A., Mohammadi, M., Khalili, H., Malayeri, A., 2020. Crocin: a protective natural antioxidant against pulmonary fibrosis induced by bleomycin. Pharmacol. Rep. 72, 992–1001. https://doi.org/10.1007/s43440-019-00023-y.

Mohammadi, G., Korani, M., Nemati, H., Nikpoor, A.R., Rashidi, K., Varmira, K., Abbasifard, M., Kesharwani, P., Korani, S., Sahebkar, A., 2022. Crocin-loaded nanoliposomes: Preparation, characterization, and evaluation of anti-inflammatory effects in an experimental model of adjuvant-induced arthritis. J. Drug Deliv. Sci. Tec. 74, 103618. https://doi.org/10.1016/j.jddst.2022.103618.

Prieložná, J., Mikušová, V., Mikuš, P.J.I.J., 2024. Advances in the delivery of anticancer drugs by nanoparticles and chitosan-based nanoparticles. Int.J Pharm-X 8, 100281. https://doi.org/10.1016/j.ijpx.2024.100281.

Rawat, P.S., Jaiswal, A., Khurana, A., Bhatti, J.S., Navik, U., 2021. Doxorubicin-induced cardiotoxicity: an update on the molecular mechanism and novel therapeutic strategies for effective management. Biomed. Pharmacother. 139, 111708. https://doi.org/10.1016/j.biopha.2021.111708.

Robert Li, Y., Traore, K., Zhu, H., 2024. Novel molecular mechanisms of doxorubicin cardiotoxicity: latest leading-edge advances and clinical implications. Mol. Cell. Biochem. 479, 1121–1132. https://doi.org/10.1007/s11010-023-04783-3.

Saravani, R., Sargazi, S., Saravani, R., Rabbani, M., Rahdar, A., Taboada, P., 2020. Newly crocin-coated magnetite nanoparticles induce apoptosis and decrease VEGF expression in breast carcinoma cells. J. Drug Deliv. Sci. Tec. 60, 101987. https://doi.org/10.1016/j.jddst.2020.101987.

Schussler, O., Chachques, J.C., Alifano, M., Lecarpentier, Y., 2022. Key roles of RGD-recognizing integrins during cardiac development, on cardiac cells, and after myocardial infarction. J. Cardiovasc. Transl. 15, 179–203. https://doi.org/10.1007/s12265-021-10154-4.

Sheibani, M., Azizi, Y., Shayan, M., Nezamoleslami, S., Eslami, F., Farjoo, M.H., Dehpour, A.R., 2022. Doxorubicin-induced cardiotoxicity: an overview on pre-clinical therapeutic approaches. Cardiovasc. Toxicol. 22, 292–310. https://doi.org/10.1007/s12012-022-09721-1.

Singh, M., Kadhim, M.M., Turki Jalil, A., Oudah, S.K., Aminov, Z., Alsaikhan, F., Jawhar, Z.H., Ramírez-Coronel, A.A., Farhood, B., 2023. A systematic review of the protective effects of silymarin/silibinin against doxorubicin-induced cardiotoxicity. Cancer Cell Int. 23, 88. https://doi.org/10.1186/s12935-023-02936-4.

Soltani, M., Farhadi, A., Rajabi, S., Homayouni-Tabrizi, M., Hussein, F.S., Mohammadian, N., 2024. Folic acid-modified nanocrystalline cellulose for enhanced delivery and anti-cancer effects of crocin. Sci. Rep. 14, 13985. https://doi.org/10.1038/s41598-024-64758-2.

Swildens, J., de Vries, A.A., Li, Z., Umar, S., Atsma, D.E., Schalij, M.J., van der Laarse, A., 2011. Integrin stimulation favors uptake of macromolecules by cardiomyocytes in vitro. Cell. Physiol. Biochem. 26, 999–1010. https://doi.org/10.1159/000324013.

Szponar, J., Niziński, P., Dudka, J., Kasprzak-Drozd, K., Oniszczuk, A., 2024. Natural Products for Preventing and Managing Anthracycline-Induced Cardiotoxicity: a Comprehensive Review. Cells 13, 1151. https://doi.org/10.3390/cells13131151.

Taghizadeh, F., Mehryab, F., Mortazavi, S.A., Rabbani, S., Haeri, A.J., 2023. Thiolated chitosan hydrogel-embedded niosomes: a promising crocin delivery system toward the management of aphthous stomatitis. Carbohydr. Polym. 318, 121068. https://doi.org/10.1016/j.carbpol.2023.121068.

Tavasoli, S., Borjizadeh, Z., Anvar, A., Ahari, H., Moradi, S., Jafari, S.M., 2023. Crocin-loaded nanocarriers; approaches and applications. Curr. Opin. Food Sci. 101099. https://doi.org/10.1016/j.cofs.2023.101099.

van der Zanden, S.Y., Qiao, X., Neefjes, J., 2021. New insights into the activities and toxicities of the old anticancer drug doxorubicin. FEBS J. 288, 6095–6111. https://doi.org/10.1111/febs.15583.

Wang, L., Cao, Y., Zhang, X., Liu, C., Yin, J., Kuang, L., He, W., Hua, D., 2022. Reactive oxygen species-responsive nanodrug of natural crocin-i with prolonged circulation for effective radioprotection. Colloid. Surface. B 213, 112441. https://doi.org/10.1016/j.colsurfb.2022.112441.

Wang, M., Wang, Y., Mu, Y., Yang, F., Yang, Z., Liu, Y., Huang, L., Liu, S., Guan, X., Xie, Z., Gu, Z., 2023. Engineering SIRPα cellular membrane-based nanovesicles for combination immunotherapy. Nano Res. 16, 7355–7363. https://doi.org/10.1007/s12274-023-5397-4.

Wong, K.H., Xie, Y., Huang, X., Kadota, K., Yao, X.S., Yu, Y., Chen, X., Lu, A., Yang, Z., 2020. Delivering Crocetin across the Blood-Brain Barrier by using gamma-Cyclodextrin to Treat Alzheimer's Disease. Sci. Rep. 10, 3654. https://doi.org/10.1038/s41598-020-60293-y.

Wu, R., Wang, H.-L., Yu, H.-L., Cui, X.-H., Xu, M.-T., Xu, X., Gao, J.-P., 2016. Doxorubicin toxicity changes myocardial energy metabolism in rats. Chem. Biol. Interact. 244, 149–158. https://doi.org/10.1016/j.cbi.2015.12.010.

Xi, L., Qian, Z., Du, P., Fu, J., 2007. Pharmacokinetic properties of crocin (crocetin digentiobiose ester) following oral administration in rats. Phytomedicine 14, 633–636. https://doi.org/10.1016/j.phymed.2006.11.028.

Yarmohammadi, F., Rezaee, R., Karimi, G., 2021. Natural compounds against doxorubicin-induced cardiotoxicity: a review on the involvement of Nrf2/ARE signaling pathway. Phytother. Res. 35, 1163–1175. https://doi.org/10.1002/ptr.6882.

Yoshino, F., Yoshida, A., Umigai, N., Kubo, K., Masaichi, C.I.L., 2011. Crocetin reduces the oxidative stress induced reactive oxygen species in the stroke-prone spontaneously hypertensive rats (SHRSPs) brain. J. Clin. Biochem. Nutr. 49, 182–187. https://doi.org/10.3164/jcbn.11-01.

You-Ling, M., Rui, Z., Shi-Ying, L., Zhang, Z.-Y., Mei-Fei, Z., Qian, L., 2023. Crocetin protects cardiomyocytes against hypoxia/reoxygenation injury by attenuating Drp1-mediated mitochondrial fission via PGC-1α. J. Geriatr. Cardiol. 20, 68. https://doi.org/10.26599/1671-5411.2023.01.001.

Zhang, S., Liu, X., Bawa-Khalfe, T., Lu, L.-S., Lyu, Y.L., Liu, L.F., Yeh, E.T., 2012. Identification of the molecular basis of doxorubicin-induced cardiotoxicity. Nat. Med. 18, 1639–1642. https://doi.org/10.1038/nm.2919.

Zhang, H., Lin, J., Shen, Y., Pan, J., Wang, C., Cheng, L., 2022. Protective effect of crocin on immune checkpoint inhibitors-related myocarditis through inhibiting NLRP3 mediated pyroptosis in cardiomyocytes via NF-κB pathway. J. Inflamm. Res. 1653–1666. https://doi.org/10.2147/JIR.S348464.

Zhang, S., Zhang, Q., Lu, Y., Chen, J., Liu, J., Li, Z., Xie, Z., 2024. Roles of Integrin in Cardiovascular Diseases: from Basic Research to Clinical Implications. Int. J. Mol. Sci. 25, 4096. https://doi.org/10.3390/ijms25074096.

Zhao, Z., Jiang, S., Fan, Q., Xu, K., Xu, Y., Wu, F., Zhang, X., Wang, T., Xia, Z., 2023. Apocynum venetum leaf extract alleviated doxorubicin-induced cardiotoxicity by regulating organic acid metabolism in gut microbiota. Front. Pharmacol. 14, 1286210. https://doi.org/10.3389/fphar.2023.1286210.